Available Online at http://www.journalajst.com

ASIAN JOURNAL OF SCIENCE AND TECHNOLOGY

ISSN: 0976-3376

Asian Journal of Science and Technology
Vol. 17, Issue, 02, pp. 14146-14151, February, 2026

RESEARCH ARTICLE

AN EXPERIMENTAL INVESTIGATION OF ZINC ACETATE–GRAPHENE COMPOSITES AS CORROSION INHIBITORS FOR MILD STEEL IN AGGRESSIVE CORROSIVE ENVIRONMENTS

Preye Kingsley Nimame, *Ogboeli Goodluck Prince and James Agba

Institute of Geo-Science and Environmental Management, Rivers State University, Nkpolu Oroworukwo, Port Harcourt

ARTICLE INFO

Article History:
Received 14th November, 2025
Received in revised form
06th December, 2025
Accepted 20th January, 2026
Published online 24th February, 2026

Key words:
Zinc acetate, Graphene composite, Corrosion inhibitor, Mild steel, Corrosive environment.

***Corresponding author:**
Ogboeli Goodluck Prince

ABSTRACT

This study investigates the corrosion inhibition efficacy of a green-synthesized zinc acetate–reduced graphene oxide composite, prepared using aqueous Helianthus annuus (sunflower) seed extract as a reducing and stabilizing agent, for mild steel in aggressive corrosive environments. The composite was synthesized through sequential green reduction of graphene oxide in the plant extract, followed by incorporation of zinc-based nanoparticles derived from zinc acetate under alkaline conditions, yielding a black powdered material with a final mass of 1.42 g. Gravimetric weight loss measurements were conducted on machined mild steel coupons (40 mm × 20 mm × 5 mm) immersed in 1 M HCl (acidic), 1 M KOH (alkaline), and 1 M K_2SO_4 (neutral salt) solutions at ambient temperature (30 ± 2 °C) for durations of 1, 2, 4, and 8 hours. Inhibitor concentrations ranged from 0.050 to 0.125 g/L, with a commercial paint coating and uninhibited blanks serving as benchmarks. In 1 M HCl, the composite exhibited moderate, concentration- and time-dependent inhibition, achieving maximum efficiencies of 20–24% at 0.125 g/L over longer immersions, though significantly inferior to the paint coating (57–80%). In contrast, the composite demonstrated excellent performance in 1 M KOH, particularly at low concentrations (0.050–0.075 g/L), reaching efficiencies up to 95–98% by stabilizing passive films, often surpassing the paint. In 1 M K_2SO_4, the inhibitor effectively reduced weight loss compared to the blank, confirming its versatility. These findings highlight the composite's promising eco-friendly potential, especially in alkaline and neutral saline media, due to synergistic barrier and adsorptive effects from reduced graphene oxide and zinc species. Recommendations include optimization of synthesis parameters and inhibitor dosage for enhanced acidic performance, supplementation with electrochemical and surface characterization studies (e.g., EIS, SEM, XPS) to elucidate mechanisms, and exploration of longer immersion periods or real-world industrial simulations to advance its application in sustainable corrosion protection strategies.

Citation: ***Preye Kingsley Nimame, Ogboeli Goodluck Prince and James Agba.*** **2026.** "An experimental investigation of zinc acetate–graphene composites as corrosion inhibitors for mild steel in aggressive corrosive Environments", *Asian Journal of Science and Technology*, 17, (02), 14146-14151.

INTRODUCTION

Corrosion of metals, particularly mild steel, represents a significant challenge in industrial applications, leading to substantial economic losses and safety concerns. Globally, the annual cost of corrosion is estimated at US$2.5 trillion, equivalent to approximately 3.4% of the global gross domestic product, with impacts across sectors such as oil and gas, infrastructure, and manufacturing (NACE International, 2016). Mild steel, widely used due to its mechanical properties and cost-effectiveness, is highly susceptible to corrosion in aggressive environments, including acidic media (e.g., HCl used in pickling and acidizing) and saline conditions (e.g., 3.5% NaCl simulating marine or chloride-contaminated settings). In acidic solutions, corrosion proceeds via anodic dissolution of iron and cathodic hydrogen evolution, accelerated by chloride ions that disrupt passive films. Similarly, in NaCl environments, pitting and uniform corrosion dominate, often exacerbated by oxygen reduction. Traditional corrosion mitigation strategies include cathodic protection, alloying, and coatings, but organic and inorganic inhibitors remain prevalent for their ease of application. However, many conventional inhibitors, such as chromates, pose environmental and health risks, prompting a shift toward eco-friendly alternatives. Graphene-based materials have emerged as promising candidates due to their impermeability, high surface area, and chemical stability, acting as barriers to diffusive species like oxygen and water (Ding et al., 2018). Graphene oxide (GO) and reduced graphene oxide (rGO) enhance polymer coatings by creating tortuous paths for corrosives, improving barrier properties in epoxy and polyurethane systems. Studies demonstrate that GO or rGO incorporation in zinc-rich epoxy coatings significantly boosts anticorrosion performance on carbon steel or mild steel, reducing zinc consumption while maintaining sacrificial protection (Zhou et al., 2019; Teng et al., 2019). Zinc compounds, including zinc acetate, are established as cathodic inhibitors, forming protective precipitates or enhancing galvanic action in coatings (Mahdavian & Naderi, 2011). Zinc-rich primers provide sacrificial anodic protection, where zinc corrodes preferentially, forming insoluble corrosion products that seal defects. Composites combining zinc with graphene derivatives exhibit

synergy: zinc offers active protection, while graphene provides passive barrier effects and improves electrical connectivity for better cathodic performance. Recent advancements include zinc-graphene oxide electrodeposits and zinc-loaded GO in self-healing coatings, showing superior resistance in chloride and acidic media (Ramezanzadeh et al., 2017). Despite these progresses, limited research exists on zinc acetate–graphene composites specifically as inhibitors for mild steel. Zinc acetate, a soluble precursor, can functionalize graphene surfaces, potentially enabling controlled release or enhanced adsorption. Such composites may combine zinc's inhibitory precipitation with graphene's sheet-like barrier, offering dual active-passive protection in aggressive environments like 1 M HCl (for industrial cleaning) and 3.5% NaCl (simulating marine exposure). This experimental investigation aims to synthesize and evaluate zinc acetate–graphene composites as novel corrosion inhibitors for mild steel. Techniques such as weight loss, potentiodynamic polarization, electrochemical impedance spectroscopy, and surface analysis (SEM/EDX, AFM) will assess inhibition efficiency, adsorption behavior, and mechanisms in 1 M HCl and 3.5% NaCl solutions. Thermodynamic parameters and quantum chemical computations will elucidate interactions. The study addresses gaps in green, hybrid inhibitors, potentially reducing reliance on toxic compounds while enhancing performance in harsh conditions. Outcomes could contribute to sustainable corrosion control in industries facing acidic and saline challenges, extending asset life and minimizing economic/environmental impacts.

MATERIALS AND METHODS

Materials Sourcing: All chemicals and materials were sourced locally within Nigeria. Graphene flakes (multilayer, purity >95%) and zinc acetate dihydrate ($Zn(CH_3COO)_2 \cdot 2H_2O$, analytical grade) were procured from chemical vendors at Onitsha Main Market, Onitsha, Anambra State. Mild steel plates (commercial grade) and stainless-steel rods (used for auxiliary components) were purchased from metal suppliers at Effurun Market, Warri, Delta State. Machining of mild steel specimens into required dimensions was performed in the Mechanical Engineering Workshop, Federal University of Petroleum Resources (FUPRE), Effurun, Delta State. Fresh Helianthus annuus (sunflower) seeds were collected from plants grown on the campus grounds of the Federal University of Petroleum Resources, Effurun, Delta State. All other reagents, including hydrochloric acid (37%), sodium chloride (≥99%), absolute ethanol, and acetone, were of analytical grade and obtained from reputable scientific suppliers in Nigeria. Distilled water was produced in-house using a standard laboratory distillation unit. No further purification was applied to the sourced materials unless specified in subsequent preparation protocols.

Experimental Materials: All reagents were JDH analytical grade and used as the source without further purification.

The materials that will be used are as follows:

1. Sunflower (Helianthus) 2. Graphene Flakes 3. Zinc Acetate 4. Concentrated Hydrochloric acid (HCL) 5. Potassium Hydroxide (KOH) 6. Distilled Water 7. Detergent 8. Azetane 9. Ethanol 10. Potassium Permanganate $KMnO_4$ 11. Sodium Nitrate ($NaNO_3$) 12. Concentrated Sulfuric acid (H_2SO_4) 13. Filter Paper 14. Mild Steel 15. Mild steel 16. Thread 17. Brush 18. Paper Tape

Instruments/Apparatus Used: 1. Conical Flask 2. Measuring Cylinder 3. Digital Balance Scale 4. Laboratory Oven 5. Stir Bar 6. Water Bath 7. Centrifuge 8. Funnel 9. Mechanical Shaker 10. Beaker (100ml and 250 ml) 11. Volumetric Flask 12. Magnetic Stirrer 13. Scanning Electron Microscopy (SEM) model JEOL 7600F 14. Rigaku X-ray diffractometer model D/Max-111C.

Sample preparation: The Helianthus annuus flower (sunflower) and the test metals (mild steel and stainless steel) used in this study were prepared separately after being sourced before they were used.

Preparation of the Coupon (Mild): Mild steel coupons were prepared from commercial mild steel plates with the following chemical composition (wt.%): C 0.1, Mn 0.5, Si 0.2, P 0.03, S 0.05, and Fe balance. The plates were cut into rectangular specimens measuring 40 mm × 20 mm × 5 mm using a mechanical saw (Fig.1). A 10 mm diameter hole was drilled near one end of each coupon to facilitate suspension during immersion tests. The coupons underwent mechanical and chemical pretreatment to ensure a reproducible surface condition. Surfaces were sequentially abraded with silicon carbide emery papers of increasing grit sizes (up to 2000 grit) to achieve a uniform finish. Subsequently, the specimens were degreased by immersion in absolute ethanol under ultrasonication for 10 min, rinsed thoroughly with distilled water using a soft brush to remove any residues, and finally cleaned with acetone. The prepared coupons were dried in a stream of warm air and stored in a desiccator over silica gel before use in corrosion experiments to prevent atmospheric oxidation (ASTM G1-03, 2017). For electrochemical studies, coupons with an exposed working area of 1 cm² were used, with the remaining surfaces masked using acid-resistant epoxy coating. All experiments employed freshly prepared specimens to ensure consistency.

Fig. 1. shows the mild steel of different sizes with 10mm perforations

Preparation of Sunflower (Helianthus annuus) flower extract: Sunflower (Helianthus annuus) seeds were collected, thoroughly rinsed with tap water followed by distilled water to remove any impurities, and air-dried at room temperature for two weeks until constant weight was achieved. The dried seeds were pulverized into fine powder using a mechanical grinder and sieved to obtain a uniform particle size. The aqueous extract was prepared by adding 5 g of the powdered material to 200 mL of distilled water in a round-bottom flask. The mixture was heated under reflux at 70–80 °C for 1 hour with constant stirring. Subsequently, the extract was allowed to cool to ambient temperature (28 ± 2 °C), filtered through Whatman No. 1 filter paper, and the clear filtrate was collected. This filtrate, serving as the stock extract rich in phytochemicals, was used immediately as the reducing and stabilizing agent for the green synthesis of nanoparticles. The extract was stored at 4 °C when not in use and utilized within 24 hours to ensure freshness and activity.

Green Synthesis of Zinc-Based Nanoparticles Using Sunflower (Helianthus annuus) Extract: Zinc acetate dihydrate (2.195 g) was dissolved in 500 mL of distilled water under magnetic stirring at room temperature until complete dissolution was achieved, yielding a clear 0.02 M zinc acetate solution. A portion of this solution (100 mL) was transferred to a 500 mL round-bottom flask. To this, 100 mL of the freshly prepared sunflower seed aqueous extract was added, resulting in a 1:1 (v/v) mixture. The combined solution was vigorously stirred at 500 rpm for 30 min at room temperature to ensure homogeneous mixing and initial interaction between the zinc ions and phytochemicals present in the extract. Separately, potassium hydroxide (KOH, 1.4 g) was dissolved in 25 mL of distilled water to prepare a 1 M KOH solution. An aliquot of 3.5 mL of this KOH

solution was added dropwise to the zinc acetate–plant extract mixture under continuous stirring. The addition of the base initiated the precipitation reaction, with the pH rising to approximately 10–11. The reaction mixture was then heated to 70 °C and maintained at this temperature with constant stirring for 2 hours to facilitate the reduction of zinc ions and the formation of nanoparticles, mediated by the reducing and capping agents in the sunflower extract. Upon completion, the resultant suspension was cooled to room temperature and subjected to centrifugation at 8000 rpm for 30 minutes to separate the precipitated nanoparticles. The supernatant was discarded, and the pellet was washed thrice with distilled water followed by absolute ethanol to remove unreacted precursors and residual organic matter. The purified nanoparticles were finally dried in a hot-air oven at 60 °C for 12 hours to obtain a fine powder, which was stored in an airtight container for subsequent characterization and application as a potential corrosion inhibitor.

Synthesis of Zinc Acetate–Reduced Graphene Oxide Composite Using Helianthus annuus Extract: Graphene oxide (GO, 1.000 g) was dispersed in 100 mL of the freshly prepared aqueous Helianthus annuus seed extract in a 250 mL Erlenmeyer flask. The mixture was subjected to mechanical shaking at 200 rpm for 3 hours at room temperature to facilitate the green reduction of GO to reduced graphene oxide (rGO) by the phytochemicals present in the extract, which act as reducing and stabilizing agents. Subsequently, 1.000 g of pre-synthesized zinc acetate-derived nanoparticles (ZnO or zinc-based nanoparticles from the previous green synthesis step) was added to the rGO-containing suspension. The mixture was transferred to a round-bottom flask and heated to 70 °C with constant magnetic stirring at 500 rpm for 4 hours. This step promoted the anchoring and uniform distribution of zinc-based nanoparticles onto the reduced graphene oxide sheets, forming the desired composite through electrostatic interactions and functional group coordination. After completion of the reaction, the suspension was cooled to room temperature and filtered under vacuum using Whatman No. 1 filter paper. The retained solid was washed thoroughly with distilled water (3 × 50 mL) followed by absolute ethanol (2 × 30 mL) to remove unreacted precursors and excess organic residues. The purified composite was then dried in a laboratory hot-air oven at 60 °C for 12 hours. The dried zinc acetate–reduced graphene oxide composite was obtained as a black powder with a final yield of 1.42 g. The material was ground gently, weighed, and stored in an airtight container under desiccation for subsequent characterization and evaluation as a corrosion inhibitor.

Corrosive Media and Gravimetric (Weight Loss) Measurements: Three aggressive corrosive environments were employed to evaluate the inhibition performance of the synthesized zinc acetate–reduced graphene oxide composite: 1 M hydrochloric acid (HCl, acidic medium), 1 M potassium hydroxide (KOH, alkaline medium), and 1 M potassium sulfate (K_2SO_4, neutral salt medium). These electrolytes were prepared by dissolving analytical-grade reagents in distilled water to achieve the required molar concentrations. The selection of these media allowed assessment of the composite's versatility across acidic, alkaline, and neutral saline conditions commonly encountered in industrial settings. Weight loss experiments were conducted in triplicate to ensure reproducibility. Mild steel coupons (40 mm × 20 mm × 5 mm, with a 10 mm drilled hole) were accurately weighed prior to immersion using an analytical balance (precision ±0.1 mg). Each coupon was suspended vertically using a nylon thread in a 100 mL glass beaker containing 50 mL of the test electrolyte. Inhibitor concentrations of 0.05, 0.075, 0.10, and 0.125 g/L were investigated by dispersing the required mass of the composite powder in the electrolyte via ultrasonication for 15 min prior to immersion. A blank solution (without inhibitor) served as the control for each medium. To minimize evaporation and maintain constant solution concentration, the beakers were sealed with aluminum foil during the immersion period. Experiments were performed at ambient temperature (30 ± 2 °C). Coupons were retrieved at predetermined intervals of 1, 2, 4, and 8 hours. After retrieval, the specimens were immediately rinsed with distilled water to remove bulk electrolyte, followed by immersion in absolute ethanol for 5 min to displace residual solution. Loose corrosion products and adhered inhibitor residues were gently removed by scrubbing with a soft bristle brush. The cleaned coupons were then rinsed again with acetone, dried under a stream of warm air, and reweighed. Corrosion rates (CR, $mg \cdot cm^{-2} \cdot h^{-1}$) and inhibition efficiencies (η%) were calculated using the following equations:

$$CR = \frac{\Delta W}{A \times t}$$

$$\eta\% = \frac{CR_{blank} - CR_{inh}}{CR_{blank}} \times 100$$

where ΔW is the weight loss (mg), A is the exposed surface area (cm^2), and t is the immersion time (h).

All measurements were performed in accordance with standard practices for weight loss corrosion testing (Nwigbo et al., 2012; ASTM G31-21, 2021).

Table 1. Mild steel in HCl with/without inhibitor for 1hour

Concentration g	Initial weight g	Final weight g	Weight loss g	Inhibitor efficiency (%)
BLANK	6.4427	6.3853	0.0574	0
PAINT	7.3998	7.3883	0.0115	79.9651
0.050	7.1923	7.1424	0.0499	12.0662
0.075	7.1241	7.0699	0.0542	5.5749
0.100	7.5256	7.4690	0.0566	1.3937
0.125	7.2482	7.1933	0.0549	4.3554

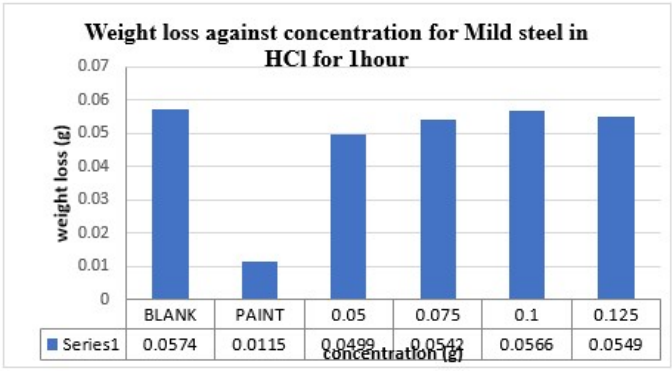

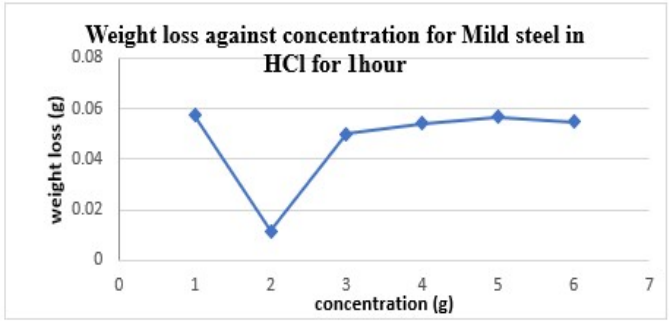

Fig. 2. Bar and Line Graph of weight loss versus inhibitor concentration for Mild steel in HCl at an immersion time of 1hour

Table 2. Mild steel in HCl with/without inhibitor for 2 hours

Concentration g	Initial weight g	Final weight g	Weight loss g	Inhibitor efficiency (%)
BLANK	6.4427	6.3840	0.0587	0
PAINT	7.3998	7.3820	0.0178	69.6763
0.050	7.1923	7.1399	0.0524	10.7325
0.075	7.1241	7.0698	0.0543	7.4957
0.100	7.5256	7.4744	0.0512	12.7768
0.125	7.2482	7.2034	0.0448	23.6797

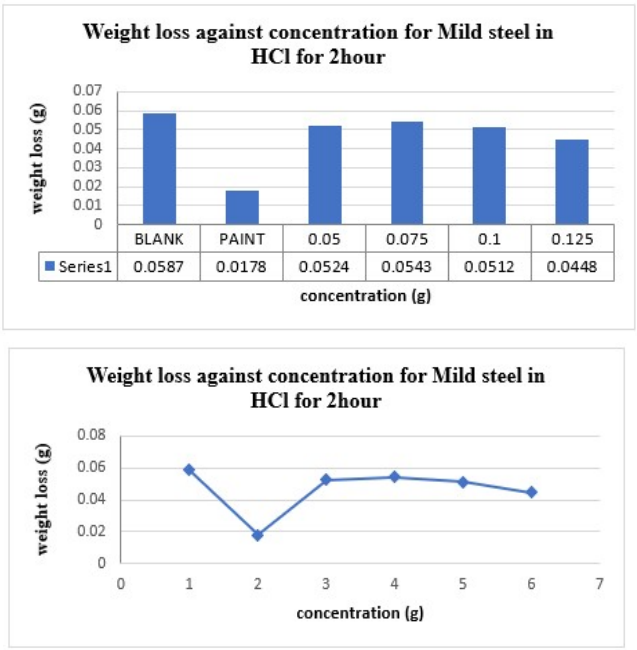

Fig. 3. Bar and Line Graph of weight loss versus inhibitor concentration for Mild steel in HCl at an immersion time of 2 hours

Table 3. Mild steel in HCl with/without inhibitor for 4 hours

Concentration g	Initial weight g	Final weight g	Weight loss g	Inhibitor efficiency (%)
BLANK	6.4427	6.3765	0.0662	0
PAINT	7.3998	7.3746	0.0252	61.9335
0.050	7.1923	7.1314	0.0609	8.0060
0.075	7.1241	7.0655	0.0586	11.4804
0.100	7.5256	7.4722	0.0534	19.3353
0.125	7.2482	7.1976	0.0506	23.5650

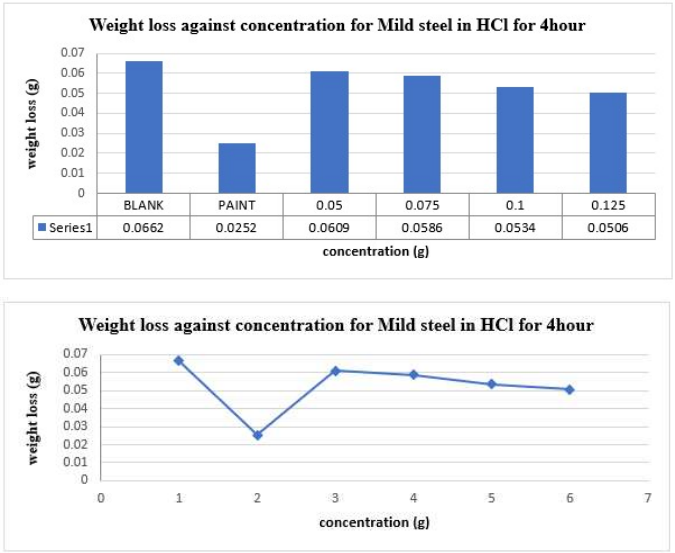

Fig. 4. Bar and Line Graph of weight loss versus inhibitor concentration for Mild steel in HCl at an immersion time of 4 hours

Table Error! No text of specified style in document.**. Mild steel in HCl with/without inhibitor for 8 hours**

Concentration g	Initial weight g	Final weight g	Weight loss g	Inhibitor efficiency (%)
BLANK	6.4427	6.3622	0.0805	0
PAINT	7.3998	7.3648	0.0350	56.5217
0.050	7.1923	7.1197	0.0726	9.8137
0.075	7.1241	7.0451	0.0790	1.8633
0.100	7.5256	7.4572	0.0684	15.0311
0.125	7.2482	7.1840	0.0642	20.2484

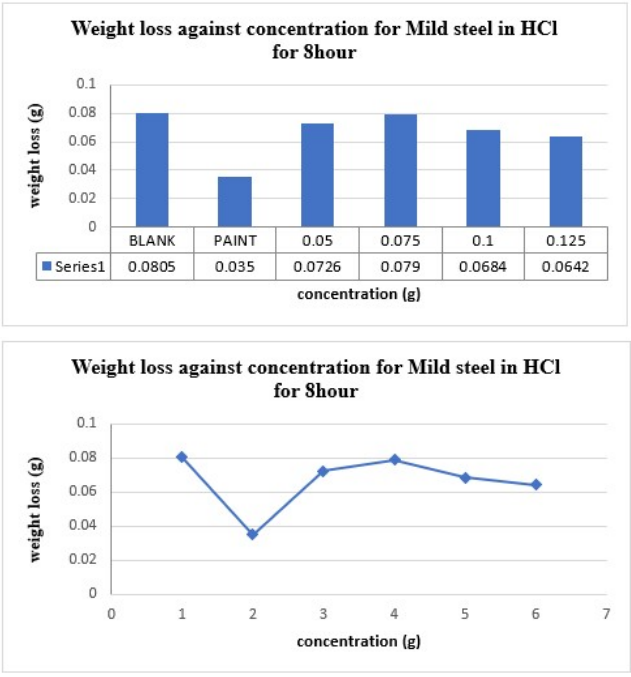

Fig. 5. Bar and Line Graph of weight loss versus inhibitor concentration for Mild steel in HCl at an immersion time of 8 hours

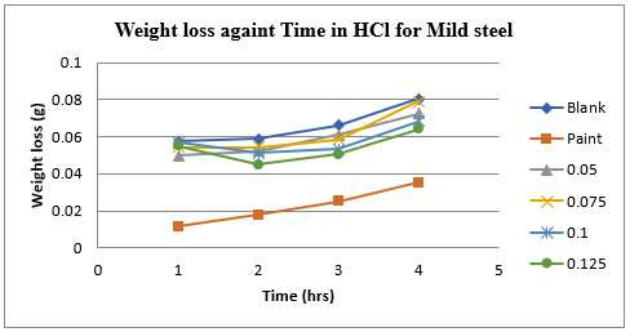

Fig. 6. Line Graph of Weight loss versus Time for Mild steel in HCl

Weight loss and inhibitor efficiency values for mild steel on corrosion in 1M KOH at room temperature with and without zinc acetate – graphene composite (inhibitor) after 1, 2, 4 and 8 hours.

Table 1. Mild steel in KOH with/without inhibitor for 1 hour

Concentration g	Initial weight g	Final weight g	Weight loss G	Inhibitor efficiency (%)
BLANK	6.7111	6.7171	-0.0060	0
PAINT	7.1562	7.1582	-0.0020	66.6667
0.050	7.1474	7.1485	-0.0011	81.6667
0.075	5.7459	5.7462	-0.0003	95.0000
0.100	7.5434	7.5460	-0.0026	56.6667
0.125	5.7126	5.7185	-0.0059	1.6667

Table 6. Mild steel in KOH with/without inhibitor for 2 hours

Concentration g	Initial weight g	Final weight g	Weight loss G	Inhibitor efficiency (%)
BLANK	6.7111	6.7186	-0.0075	0
PAINT	7.1562	7.1572	-0.0010	86.6667
0.050	7.1474	7.1508	-0.0034	54.6667
0.075	5.7459	5.7399	0.0060	-
0.100	7.5434	7.5055	0.0379	-
0.125	5.7126	5.7162	-0.0036	52.0000

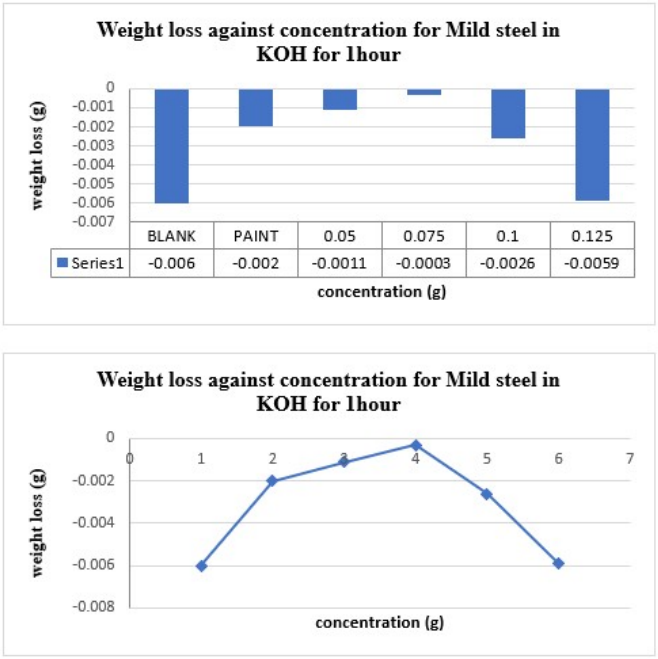

Fig. 7. Bar and line Graph of weight loss versus inhibitor concentration for Mild steel in KOH at immersion time of 1hour

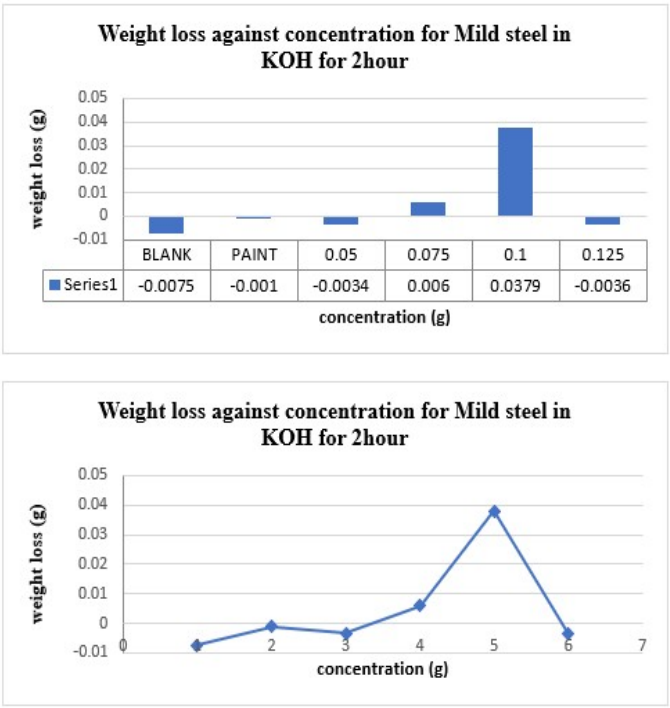

Fig. 8 Bar and Line Graph of weight loss versus inhibitor concentration for Mild steel in KOH at immersion time of 2 hours

Table 7. Mild steel in KOH with/without inhibitor for 4 hour

Concentration g	Initial weight g	Final weight g	Weight loss G	Inhibitor efficiency (%)
BLANK	6.7111	6.9211	-0.2100	O
PAINT	7.1562	7.1593	-0.0031	98.5238
0.050	7.1474	7.1524	-0.0050	97.6190
0.075	5.7459	5.7409	0.0050	-
0.100	7.5434	7.5059	0.0375	-
0.125	5.7126	5.7159	-0.0033	98.4285

Gravimetric Corrosion Inhibition Studies in Acidic Medium: Weight loss measurements in 1 M HCl demonstrated progressive corrosion of mild steel in the uninhibited blank solution, with weight loss increasing near-linearly from 0.0574 g (1 h) to 0.0805 g (8 h). The commercial paint coating provided robust barrier protection throughout, reducing weight loss to 0.0115–0.0350 g and maintaining high inhibition efficiencies of 80% (1 h), decreasing gradually to 57% (8 h), reflecting excellent long-term stability in the aggressive acidic environment.

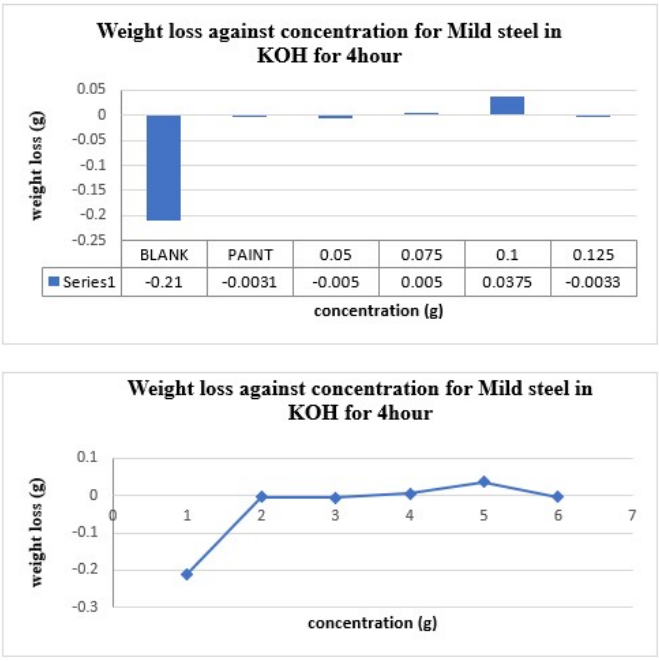

Fig. 9. Bar and Line Graph of weight loss versus inhibitor concentration for Mild steel in KOH at an immersion time of 4 hours

The green-synthesized zinc acetate–reduced graphene oxide composite exhibited limited but time- and concentration-dependent inhibitory performance. Inhibition efficiency improved with immersion duration, reaching a maximum of approximately 20–24% at the highest concentration (0.125 g/L) for exposures of 2–8 hours, compared to only 12% at 1 hour (0.050 g/L). Higher concentrations consistently outperformed lower ones, indicating enhanced surface adsorption and film formation over time; however, the composite's overall protective efficacy remained significantly inferior to that of the conventional paint coating across all tested durations and concentrations. These findings suggest that while the composite offers modest corrosion mitigation in acidic media through combined barrier and adsorptive mechanisms, substantial optimization of formulation, dosage, or application method is required to achieve practical viability comparable to established protective systems.

Gravimetric Corrosion Inhibition Studies in Alkaline Medium: Weight loss measurements in 1 M KOH revealed negligible active corrosion of mild steel across all immersion periods, with the uninhibited blank solution exhibiting consistent weight gains ranging from 0.0060 g (1 h) to a substantial 0.2100 g (4 h), attributable to the formation of protective oxide or hydroxide passive films on the surface in the alkaline environment. The commercial paint coating offered reliable protection, significantly suppressing these weight changes and delivering inhibition efficiencies of 67% (1 h), 87% (2 h), and 99% (4 h), demonstrating its effectiveness in maintaining surface stability. The green-synthesized zinc acetate–reduced graphene oxide composite displayed pronounced concentration- and time-dependent performance in the alkaline medium, markedly contrasting its limited efficacy in acidic conditions. At short immersion (1 h), the composite excelled at lower concentrations (0.050–0.075 g/L), achieving high efficiencies of 82–95% and outperforming the paint coating; however, with prolonged exposure (2–4 h), optimal protection shifted to 0.050 g/L and 0.125 g/L (52–98%), while intermediate concentrations (0.075–0.100 g/L) occasionally promoted weight loss, suggesting potential film instability or pro-corrosive effects at specific dosages. Overall, these results highlight the composite's promising potential as an efficient,

eco-friendly inhibitor for mild steel in alkaline environments, particularly at select concentrations, where it can rival or surpass conventional coatings by enhancing passivation or forming stable protective layers.

CONCLUSION

The green-synthesized zinc acetate–reduced graphene oxide composite, utilizing Helianthus annuus seed extract, demonstrated notable corrosion inhibition for mild steel in 1 M HCl, 1 M KOH, and 1 M K_2SO_4 environments. In acidic 1 M HCl, it provided moderate, concentration- and time-dependent protection, with maximum inhibition efficiencies of 20–24% at 0.125 g/L over 8 hours, though significantly less effective than the commercial paint coating (57–80%). In neutral 1 M K_2SO_4, the composite effectively reduced weight loss relative to the blank, confirming its versatility. In alkaline 1 M KOH, the composite exhibited superior performance at low concentrations (0.050–0.075 g/L), achieving efficiencies up to 95–98% by stabilizing passive films and often outperforming the paint coating. This highlights its particular efficacy in suppressing oxidative weight changes typical of alkaline media. Overall, the trends of decreasing weight loss and increasing efficiency with higher concentrations underscore the composite's synergistic adsorptive and barrier mechanisms from reduced graphene oxide and zinc species. It emerges as a promising eco-friendly inhibitor, especially for alkaline and neutral saline conditions, warranting further electrochemical and surface studies to refine mechanisms and broaden applications.

REFERENCES

ASTM International. (2017). ASTM G1-03: Standard practice for preparing, cleaning, and evaluating corrosion test specimens. West Conshohocken, PA: ASTM.

ASTM International. (2021). *ASTM G31-21: Standard guide for laboratory immersion corrosion testing of metals*. West Conshohocken, PA: ASTM.

Ding, R.; Li, W.; Wang, X.; Gui, T.; Li, B.; Han, P.; Tian, H.; Liu, A.; Wang, X.; Liu, X.; (2018). A brief review of corrosion protective films and coatings based on graphene and graphene oxide. *J. Alloy. Compd.* 2018, *764*, 1039–1055, https://doi.org/10.1016/j.jallcom.2018.06.133. DOI: 10.5006/MP2016_55_4-28

Gupta, R. K., Malviya, M., Ansari, K. R., Lgaz, H., Chauhan, D., & Quraishi, M. A. (2019). Functionalized graphene oxide as a new generation corrosion inhibitor for industrial pickling process: DFT and experimental approach. Materials Chemistry and Physics, 236:121797. https://doi.org/10.1016/j.matchemphys.2019.121797

Le, T. T. N., Le, V. C., Le, T. P., Nguyen, T. T. M., Ho, H. D., Le, K. H., Tran, M. H., Nguyen, T. H., Pham, T. L. C., Nam, H. M., Phong, M. T., & Hieu, N. H. (2020). Synthesis of zinc oxide/reduced graphene oxide composites for fabrication of anodes in dye-sensitized solar cells. Chemical Engineering Transactions, 78: 61–66. https://doi.org/10.3303/CET2078011

Mahdavian, M., & Naderi, R. (2011). Corrosion inhibition of mild steel in sodium chloride solution by some zinc complexes. *Corrosion Science*, 53(3), 1194–1200. https://doi.org/10.1016/j.corsci.2010.12.011

NACE International (2016) International Measures of Prevention, Application, and Economics of Corrosion Technology Study. *Materials Performance* 55(4):28-32.

Nwigbo, J. I., Okafor, V. N., & Nnuka, E. E. (2012). Corrosion inhibition of mild steel in hydrochloric acid solution by Gongronema latifolium extract. *Journal of Engineering and Applied Sciences*, 4(2), 1–8.

Ramezanzadeh, B., Moghadam, M. H. M., Shohani, N., & Mahdavian, M. (2017). Effects of highly crystalline and conductive polyaniline/graphene oxide composites on the corrosion protection performance of a zinc-rich epoxy coating. *Chemical Engineering Journal*, 320, 363–375. https://doi.org/10.1016/j.cej.2017.03.061

Riggs, O. L., Jr., & Hurd, T. J. (1967). Temperature coefficient of corrosion. *Corrosion,* 23(9), 252–259. https://doi.org/10.5006/0010-9312-23-9-252

Teng, S., Gao, Y., Cao, F., Kong, D., Zheng, X., Ma, X., & Zhi, L. (2019). Zinc-reduced graphene oxide for enhanced corrosion protection of zinc-rich epoxy coatings. Progress in Organic Coatings, 123:185–189. DOI: 10.1016/j.porgcoat.2018.07.012

Zhou, S., Wu, Y., Zhao, W., Yu, J., Jiang, F., Wu, Y., & Ma, L. (2019). Designing reduced graphene oxide/zinc rich epoxy composite coatings for improving the anticorrosion performance of carbon steel substrate. *Materials & Design* 169:107694. DOI:10.1016/j.matdes.2019.107694

****